Non-Thermal Hydroxyapatite Coating Methods

Subjects: Biotechnology & Applied Microbiology

Contributor: Andri Riau

Polymers are widely used in many applications in the field of biomedical engineering. Among eclectic selections of polymers, those with low melting temperature (Tm < 200 degrees Celcius), such as poly(methyl methacrylate), poly(lactic-co-glycolic acid) or polyethylene, are often used in bone, dental, maxillofacial, and corneal tissue engineering as substrates or scaffolds. These polymers, however, are bioinert, lack of reactive surface functional groups, and had poor wettability, affecting their ability to promote cellular functions and biointegration with the surrounding tissue. Improving the biointegration can be achieved by depositing hydroxyapatite (HAp) on the polymeric substrates. Conventional thermal spray and vapor phase coating, including the Food and Drug Administration (FDA)-approved plasma spray technique, is not suitable for application on the low Tm polymers due to the high processing temperature, reaching more than 1000 degrees Celcius. Two non-thermal HAp coating approaches have been described in the literature, namely the biomimetic deposition and direct nanoparticle immobilization techniques. Here, we elaborate on the unique features of each technique, followed by discussing the advantages and disadvantages of each technique to help readers decide on which method is more suitable for their intended applications.

Keywords: hydroxyapatite ; coating ; polymer ; crystallinity ; tissue engineering ; calcium ; simulated body fluid

1. Introduction

It is obvious that the thermal spray and vapor deposition techniques do not apply to most polymers, let alone low T_m polymers. First, the abrasion methods in the surface preparation stage are typically harsh, intended to increase the surface area and create microscale roughness for the coating to mechanically adhere. As such, these treatments may not be well tolerated by low T_m or soft polymers. Second and the confounding factor of the techniques is the extremely high processing temperature. The high particle projection velocity may also not be able to be tolerated by the soft polymers. Other techniques that are solution-based and non-thermal at the deposition phase eventually require a calcination step to densify and crystallize the HAp coating.

2. Biomimetic Approach

The biomimetic HAp coating process overcomes many of the shortcomings of conventional thermal spray coating techniques and mimics nature's biomineralization mechanism [1]. In nature, organisms use proteins and organic materials (polymers) as templates for the formation of mineral structures, such as teeth, bones, and shells. The combination of protein and polymers control the mineralization rate, mineral phase, and orientation of HAp crystals. In humans, biomineralization typically occurs at physiological temperature (~37 °C) and neutral pH range. Researchers have extrapolated this natural mineralization method and subsequently developed a solution-based process that mimics nature's template-mediated materialization. Such an approach can be applied to any surface that interfaces with an aqueous solution. This benign, non-thermal coating process can, therefore, be easily applied to implants with pores and complex dimensions.

In 1990, Kokubo et al. demonstrated that the formation of an apatite layer on bioactive ceramics can be reproduced by incubating a substrate in simulated body fluid (SBF) in vitro [2]. SBF is a solution that has inorganic ion concentrations similar to those of human blood plasma but does not contain any cells or protein. The solution contains supersaturated levels of calcium (Ca^{2+}) and hydrogen phosphate (HPO_4^{2-}) ions. The pH of SBF is typically adjusted to 7.25–7.40 at 36.5 °C. There have been several versions of SBF, differing in the concentrations of the components and buffer solutions [2][3][4][5][6][7]. Over the years, to accelerate the mineralization process, some researchers have increased the ion concentrations of SBF to up to 10 times of the blood plasma (Table 1) [8][9][10]. Nevertheless, the majority of studies in the literature appeared to favor the uses of c-SBF (142.0 mM Na^+, 5.0 mM K^+, 1.5 mM Mg^{2+}, 2.5 mM Ca^{2+}, 147.8 mM Cl^-, 4.2 mM HCO^{3-}, 1.0 mM HPO_4^{2-}, and 0.5 mM SO_4^{2-}) and 1.5× SBF solutions.

Table 1. Composition of simulated body fluid (SBF) and its variants.

Solution	Ionic concentration (mM)								Buffer, pH	Reference
	Na^+	K^+	Mg^{2+}	Ca^{2+}	Cl^-	HCO^{3-}	HPO_4^{2-}	SO_4^{2-}		
Blood plasma	142.0	5.0	1.5	2.5	103.0	27.0	1.0	0.5	-	[3]
Original SBF	142.0	5.0	1.5	2.5	148.8	4.2	1.0	0	*Tris, 7.25–7.4	[2]
c-SBF	142.0	5.0	1.5	2.5	147.8	4.2	1.0	0.5	Tris, 7.25–7.4	[3]
r-SBF	142.0	5.0	1.5	2.5	103.0	27.0	1.0	0.5	**HEPES, 7.4	[7]
np-SBF	142.0	5.0	1.5	2.5	103.0	4.2	1.0	0.5	HEPES, 7.4	[5]
t-SBF	142.0	5.0	1.5	2.5	125.0	27.0	1.0	0.5	***dH_2O	[4]
i-SBF	142.0	5.0	1.0	1.6	103.0	27.0	1.0	0.5	HEPES, 7.4	[6]
m-SBF	142.0	5.0	1.5	2.5	103.0	10.0	1.0	0.5	HEPES, 7.4	[6]
1.5× SBF	213.0	7.5	2.3	3.8	223.0	6.3	1.5	0.75	Tris, 7.25	[9]
5× SBF	726.0	25.0	7.5	12.5	760.0	21.0	5.0	2.5	Tris, 7.4	[8]
10× SBF	1020.0	5.0	5.0	25.0	1035.0	10.0	10.0	-	dH_2O	[10]

*Tris = 2-amino-2-hydroxymethyl-propane-1,3-diol; **HEPES = 2-[4-(2-hydroxyethyl)piperazin-1-yl]ethanesulfonic acid; ***dH_2O = deionized water.

The mechanism of apatite formation in SBF is fundamentally simple and is best explained by Tanahashi and Matsuda's work that demonstrated that the apatite nucleation on a substrate in SBF is initiated by adsorption of Ca^{2+} on negatively charged surfaces, followed by the recruitment of HPO_4^{2-} via ionic interactions with Ca^{2+}, to form CaP crystals or nanoparticles (Figure 1, steps 1 and 2) [11]. Over time, the accumulation of the nanoparticles forms an apatite-like layer on the substrate (Figure 1, steps 3 and 4). The authors showed that, in decreasing order, the efficiency of apatite formation is achieved by the functionalization of substrate surfaces with $–H_2PO_4$ > –COOH > –OH > $–NH_2$ > $–CH_3$. In addition to heterogeneous nucleation on material surfaces, homogenous apatite nucleation can happen spontaneously in the SBF (Figure 1, step 5) [4]. Hence, the authors did not rule out the possibility of ionic interactions of the Ca^{2+} or PO_4^{3-} of the CaP nanoparticles with the growing apatite deposits on the substrate [11].

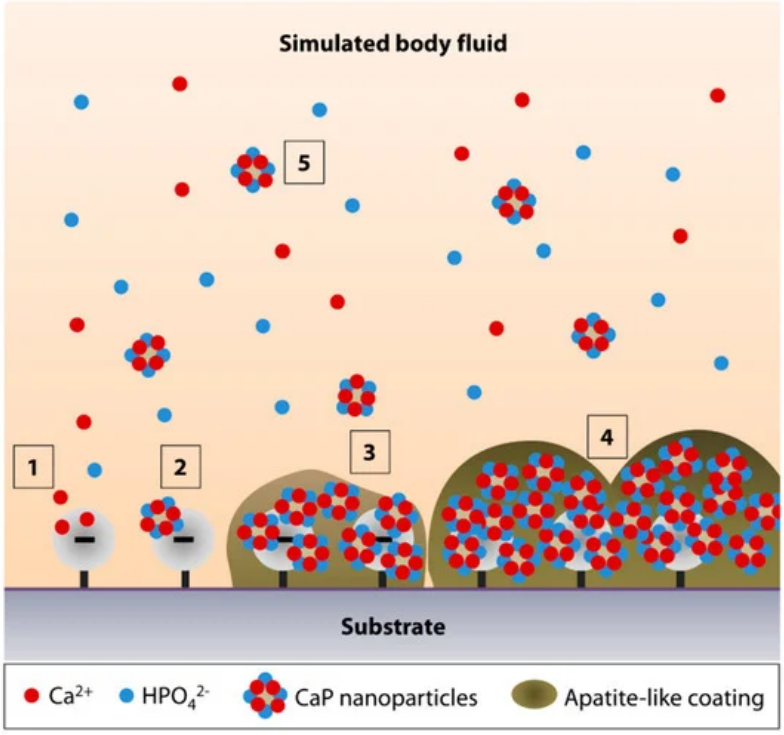

Figure 1. Simulated body fluid (SBF)-mediated mineralization on a negatively charged substrate surface. (**1**) Ionic interactions of calcium ions (Ca^{2+}) with a negatively charged surface initiate the apatite nucleation. (**2**) Accumulation of Ca^{2+} attracts the hydrogen phosphate (HPO_4^{2-}) ions. (**3**,**4**) The accumulation forms CaP nanoparticles or crystals, serving as a secondary nucleation site for continued apatite growth. (**5**) The surface nucleation site may also attract the CaP crystals that undergo homogenous nucleation in the SBF.

In light of the earlier study by Tanahashi and Matsuda [11], it is apparent that surface functionalization is required to prime the surface of most biomedical polymers to increase the efficiency of CaP deposition. A later study by Leonor et al. revealed that in addition to surface phosphorylation and carboxylation, surface functionalization with sulfonic acid ($–SO_3H$) is an alternative method to enhance apatite formation on low T_m polymers, e.g., ethylene vinyl alcohol (EVOH) and high molecular weight polyethylene (HMWPE) [12]. The sulfonated polyamide surface appeared to be more effective in driving the biomineralization process compared to the carboxylated surface [13].

2.1. Biomineralization on Phosphorylated Surface

The most common technique to functionalize the surface of polymers with phosphonate groups is by the grafting of mono(2-acryloyloxyethyl) phosphate (MAEP) or 2-(methacryloyloxy) ethyl phosphate (MOEP) [14][15][16][17][18][19]. By grafting MOEP on high-density polyethylene (HDPE), Tretinnikov and colleagues showed the formation of an apatite-like coating could be seen as early as 2 days following incubation in c-SBF at 37 °C [15]. They also revealed that to produce a coating that was close to the theoretical Ca/P ratio of HAp, grafting densities of above 2 µg/cm^2 were required [15].

Phosphonate functional groups can also be introduced by the chemical treatment of polymers. Mahjoubi et al. modified poly(D,L-lactic acid) (PDLLA) surface with phosphonate groups via diazonium chemistry [18]. The immersion in c-SBF for 2 and 4 weeks resulted in a HAp-like coating (Ca/P ratio of 1.7) that contained crystals with globular morphology, covering the entire PDLLA surface [18]. By calculating the ratio of v1(PO_4^{3-}):v(C–COO) from the Raman spectra, it was demonstrated that the coating thickness increased with incubation time in the SBF. The Fourier transfer infrared (FTIR) assessment revealed the presence of v3(CO_3^{2-}) peaks between 1400 and 1600 cm^{-1}, and v1 and v3(PO_4^{3-}) peaks between 900 and 1000 cm^{-1}, which were the IR signature of stoichiometric HAp. Both chondrogenic cell line, ATDC5, and osteoblastic cell line, MC3T3-E1, showed good biocompatibility with the HAp-coated PDLLA and higher mineral deposition rate than when cultured on the non-coated substrate. Another example of phosphorylation technique was performed by Sailaja et al. by incubating PVA films in phosphoric acid and urea [19]. After 10 days of incubation in c-SBF, layers of HAp (Ca/P ratio of 1.67) could be found on the phosphorylated PVA surface [19]. However, the X-ray diffraction (XRD) pattern of the coating suggested a poor HAp crystallinity. Nevertheless, human osteosarcoma cells were shown to attach well on the coated-PVA films and have a higher mineralization rate (higher von Kossa staining intensity) than when cultured on untreated PVA films.

2.2. Biomineralization on Carboxylated and Hydroxylated Surfaces

The other effective surface functionalizations to induce biomineralization are carboxylation and hydroxylation. Tretinnikov et al. grafted poly(acrylic acid) (PAAc) on HDPE before subjecting the HDPE to apatite deposition in c-SBF [15]. The authors found that although the deposition rate was slower than on MOEP-grafted HDPE, the Ca/P ratio of the apatite was higher (ranged between 2.2 and 2.6), suggesting an excess binding of Ca^{2+} [15]. Cui et al. showed that biomineralization in 2× SBF was more favorable on electrospun PDLLA substrate functionalized with –COOH groups or the combination of –OH and –COOH groups with a molar ratio of 3/7 or $–NH_2$, –OH and –COOH groups with a molar ratio of 2/3/5 [20]. XRD identified the coating as HAp as early as 7 days after incubation in the SBF and the crystallinity improved with longer immersion time [20]. Another example of –COOH functionalization via chemical treatment was found in studies by Wang et al. and our group [21][22]. Biomineralization was observed on PMMA, pretreated with a combination of polydopamine and 11-mercaptoundecanoic acid (11-MUA), after a 14-day incubation in 1.5× SBF (Figure 2A). In contrast to the smooth and almost featureless surface of untreated PMMA, we noted the presence of crystals with globular morphology, forming a calcium-deficient apatite layer (Ca/P ratio of 1.21 ± 0.03) on the carboxylated PMMA surface (Figure 2A,B). FTIR revealed a distinct peak at 1029 cm^{-1}, suggesting the presence of v3(PO_4^{3-}) (Figure 2C). However, two other peaks at 1147 cm^{-1} (v3(PO_4^{3-})) and 960 cm^{-1} (v1(PO_4^{3-})) that were characteristics of stoichiometric HAp (Figure 2C), could hardly be detected. A previous study has shown that low resolution of v1 and v3(PO_4^{3-}) IR bands were typically an indication of poor crystallinity of an apatite coating [23]. Using grazing incidence-X-ray diffraction (GI-XRD) at 1° grazing angle, we confirmed that the coating was indeed rather amorphous. There was a broad area under the curve, especially in the region beneath the most prominent peak at 2θ of 31.9° (Figure 2D). Another prominent peak was detected at 2θ of 26.1° (Figure 2D). According to JCPDS no. 00-026-1056, these two peaks suggested that the deposited CaP minerals were octacalcium phosphate (OCP), which was consistent with our EDX result (Figure 2B). In spite of that, the corneal stromal fibroblasts appeared to have higher attachment efficiency, proliferation, and survival rate on the coated PMMA than on the untreated surface [22].

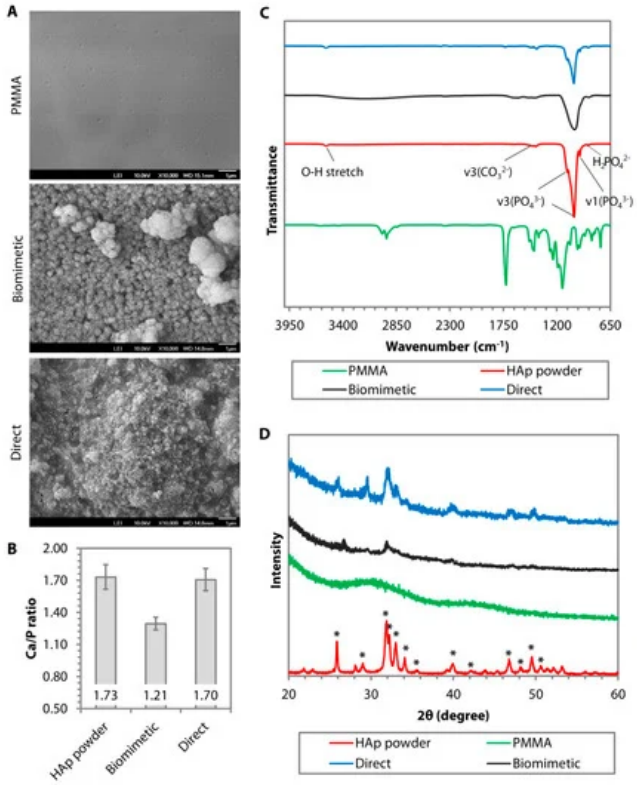

Figure 2. Comparison of surface morphology, chemical composition, phase, and crystallinity of hydroxyapatite (HAp) coating deposited on poly(methyl methacrylate) (PMMA) via biomimetic deposition or direct immobilization approach. (**A**) Scanning electron microscopy (SEM) images of PMMA surface before and after HAp coating via biomimetic deposition or direct immobilization technique. (**B**) Ca/P ratio generated from the energy dispersive X-ray (EDX) of calcined HAp (stoichiometric HAp) and the resulting CaP minerals deposited on the PMMA. (**C**) Fourier transform infrared (FTIR) patterns of uncoated PMMA (in green) and stoichiometric HAp (in red) showed a distinct IR band difference between the groups. A peak of v3(PO_4^{3-}) was found in after either biomimetic (in black) or direct (in blue) deposition. However, the other v3(PO_4^{3-}) and v1(PO_4^{3-}), which were typical of stoichiometric HAp, could only be seen in the direct deposition group. (**D**) Graze incidence-X-ray diffraction (GI-XRD) pattern revealed that the calcined HAp powder exhibited the

prominent characteristic peaks of pure HAp according to JCPDS no. 00-009-0432. Most of the peaks also appeared in the direct immobilization group. In contrast, the biomimetic group exhibited an XRD pattern of amorphous octacalcium phosphate (OCP).

Recently, Permyakova and colleagues functionalized electrospun PCL nanofibers with –COOH by using atmospheric pressure plasma copolymerization of CO_2 and C_2H_4, followed by biomineralization of the PCL in c-SBF for 21 days [24]. The authors showed a stable and linear increase in Ca concentrations over 21 days and complete coverage of the PCL nanofibers by 14 days. In contrast, the pristine PCL showed a fluctuation in the Ca concentrations and poor biomineralization over the 21-day incubation in c-SBF. There was no XRD analysis performed in the study to resolve the crystallinity of the CaP coating. The CaP coating significantly improved the adhesion and proliferation of IAR-2 epithelial cells, but not the MC3T3-E1 osteoblasts.

Hydroxylation, although not as effective as carboxylation, has also been carried out to induce biomineralization on low T_m polymers. Two of the most frequently found hydroxylation techniques in the literature are oxygen plasma treatment and chemical treatment with sodium hydroxide (NaOH) [21][22][25][26][27]. Qu et al. and our group showed that the biomineralization outcomes were similar between oxygen plasma-treated PCL and PMMA in 1.5× SBF [22][27]. Both found that the biomineralization process resulted in calcium-deficient apatite minerals with a rather poor level of crystallinity. Qu et al. further showed that OCT-1 osteoblast-like cells had a significantly better attachment efficiency and a marginally better proliferation on the coated PLGA than on the non-coated PLGA [27]. There was no difference in the alkaline phosphatase (ALP) activity between the non-coated and coated PLGA. In a separate study, Oyane et al. found that NaOH of 1M to perform surface hydrolysis on PCL was required to induce an effective biomineralization activity in c-SBF [26]. The rate of CaP deposition was commensurate with the increase of the NaOH concentration used to base hydrolyze the polymer [12]. However, GI-XRD showed that the coating had low crystallinity regardless of the NaOH concentration.

Murphy et al. attempted to perform biomineralization of poly(lactide-co-glycolide) (PLG), which surface had been pre-activated with 0.5M NaOH, in m-SBF (142.0 mM Na^+, 5.0 mM K^+, 1.5 mM Mg^{2+}, 2.5 mM Ca^{2+}, 103.0 mM Cl, 10.0 mM HCO^{3-}, 1.0 mM HPO_4^{2-}, and 0.5 mM SO_4^{2-}) for 7 days [25]. The coating resulted in calcium-deficient HAp with a Ca/P ratio of 1.55. The study did not present any in-depth surface chemistry analysis with XRD or FTIR. Human mesenchymal stem cells, seeded on the biomineralized PLG, had a higher proliferation rate, but lower ALP activity and osteocalcin production than when seeded on the pristine PLG.

2.3. Biomineralization on Peptide-bound Surface

Material-binding peptides have recently been used as non-covalent bound linkers on polymers [28][29]. The peptides can add certain functions to the polymers by permitting a further conjugation with functional molecules, such as biotin, bioactive peptides, or enzymes [28][29]. Due to the relatively recent discovery, only one example of the relevant application could be found in the literature [30]. The CaP mineralization was performed on a polymer with T_m above 200 °C. However, we can assume that the technique could also be applied to a lower T_m polymer, considering that peptides with specific binding motifs to PMMA and polycarbonate (PC) have been brought to light [31]. In the study by Iijima et al. [30], they showed that surface functionalization of polyetherimide (PEI) with peptide conjugates with sequences of PEI-binding peptide (TGADLNT-EG_2-DDD) induced biomineralization in 1.5× SBF. EG_2 or diethylene glycol unit, originated from [2-[2-(Fmoc-amino)ethoxy]ethoxy]acetic acid, is a bifunctional crosslinker that was used to link the CaP mineralization-promoting sequence (DDD) to PEI-binding peptide. However, on FTIR, only one v3(PO_4^{3-}) peak and no v1(PO_4^{3-}) peak between 1000 and 1200 cm^{-1} were detected in the apatite-like coating. The Ca/P ratio was not reported.

Utilizing the versatility of polydopamine as an adhesive molecule [32], Ghorbani et al. functionalized freeze-casted PCL scaffolds via a 24-h dip-coating in the polydopamine solution [33]. Biomineralization of the scaffolds was carried out in the c-SBF solution for 28 days under constant rotation of 30 rpm. On XRD, the existence of peaks at 2θ angle of 22.9°, 25.6°, 31.5°, 45.4°, and 56.4° confirmed the formation of HAp coating (JCPDS no. 00-09-0432), although the Ca/P ratio was only 1.46. The HAp coating resulted in significantly better adhesion, viability, and proliferation of L-929 fibroblasts, as well as better osteoinduction as evidenced by the higher level of alkaline phosphatase secretion from MG-63 cells. Substantiating the beforementioned study, Zhang et al. demonstrated that the biomineralized polydopamine-activated PCL nanofibers were also biocompatible to M3T3-E1 cells and induced better osteoconduction compared to pristine PCL [34]. In a mechanistic study, Ryu et al. showed that the terminal –OH groups of the polydopamine were responsible in initiating the biomineralization activity on various biomedical polymers, e.g., PMMA, polystyrene (PS), and polydimethylsiloxane (PDMS) [35]. XRD pattern suggested that the deposited minerals were HAp rather than OCP (JCPDS no. 00-026-1056). An innovative diffusion-controlled oxygen supply technique was employed by Perikamana et al. to functionalize PLLA nanofibers with polydopamine in a gradient manner [36]. The authors were able to demonstrate on XRD that the regions

with higher concentrations of polydopamine tended to have a higher HAp mineralization rate (JCPDS no. 00-09-0432). It is worth noting the activation of dopamine results in a brownish film on substrates and therefore, limits its application for corneal tissue engineering that typically requires transparent substrates.

3. Direct Nanoparticle Immobilization Approach

Inconsistencies in the biomineralization process in SBF, and the phase and crystallinity of the resulting CaP coating, are likely attributed to the variations in the surface functionalization techniques. The coating outcomes are also sensitive to changes in pH and temperature of the SBF solution, which undoubtedly would occur during the relatively long period of incubation time and SBF storage [37][38]. These limitations prompted us to find an alternative approach to deposit CaP nanoparticles on the surface of polymers. The approach was formulated to circumvent the surface functionalization step and significantly shorten the time to deposit the coating, as well as to utilize calcined or annealed HAp nanoparticles (to produce a coating that mimics the stoichiometric HAp). As such, the CaP coating is typically amorphous and not in the stoichiometric HAp form. Annealing the CaP deposits at a temperature of 1000 °C is necessary to produce a crystalline coating [39]. The direct immobilization technique via dip-coating was inspired by the solvent casting technique, performed by Wang and colleagues [40]. In their study, calcium-deficient hydroxyapatite (CDHA) nanocrystals, dispersed in dimethylformamide (DMF) and PLA, were deposited on a metallic substrate by solvent casting method. The CDHA was observed to be homogeneously distributed in 0.1-thick PLA films following solvent evaporation and had similar morphology and composition to natural bone mineral.

The nanoparticle immobilization was achieved via dip-coating of a polymeric substrate in an organic solution (to soften or 'liquify' the surface of the substrate to allow seeding of nanoparticles) containing HAp nanoparticles and a low amount of polymer (to increase the viscosity of the organic solution to slow the nanoparticle agglomeration and produce a more uniform coating) (Figure 3) [41]. After drying, the substrate was subjected to oxygen plasma etching for 5 min to remove surface contaminants and residual polymer that may mask the superficial layer of the coating (Figure 3). In our application, a PMMA substrate was dip-coated in chloroform containing 5% (*w/v*) of PMMA and 20% (*w/v*) of 60-nm HAp nanoparticles. We found that a single 1-min dip was optimal to coat a flat surface of PMMA sheets [41]. Coating a curved and smaller surface area of PMMA rods required multiple 5-s dips (up to 12 times) [42]. The reason behind the difference is currently unknown. The elucidation of the precise mechanism will require molecular dynamic simulations.

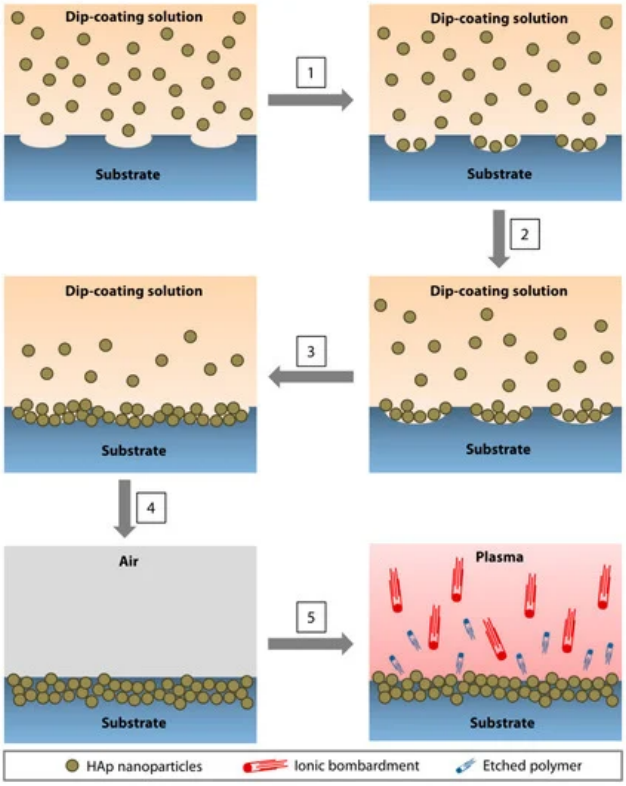

Figure 3. Direct immobilization of HAp nanoparticles via dip-coating method. (**1**) As the polymeric surface was softened by the organic solvent, pores started to form, followed by the deposition of the nanoparticles in the pores. (**2**,**3**) The pores enlarged as the dip-coating progressed and an increasing amount of nanoparticles accumulated in the cavities. (**4**) At the conclusion of the dip-coating, the substrate was air-dried. During the drying process, the 'liquified' surface began to

resolidify, immobilizing the nanoparticles near the surface of the substrate. (**5**) Oxygen plasma treatment resulted in ion bombardment of the surface, removing contaminants, and etching away the polymer that masked the nanoparticles during the drying step. An increasing amount of HAp nanoparticles emerged as the residual polymer was etched.

The dip-coating resulted in a relatively rough surface interspersed with HAp nanoparticles (Figure 2A). The resulting coating had a similar Ca/P ratio (Figure 2B) and IR pattern (Figure 2C) to the calcined HAp. Peaks attributed to O−H stretch, v3(CO_3^{2-}), v1(PO_4^{3-}), v3(PO_4^{3-}), and v(HPO_4^{2-}) could be found on both the calcined HAp and the dip-coated PMMA surface. Although it was difficult to determine the crystallinity level of the coating from the GI-XRD (due to the signal interference from the PMMA that filled the gaps between the nanoparticles), the major peaks of calcined HAp or stoichiometric HAp (JCPDS no. 00-009-0432) were noticeable on the dip-coated PMMA surface, e.g., peaks at 2θ of 25.8°, 29.0°, 31.9°, 33.0°, 34.1°, 39.9°, 46.7°, and 49.5° (Figure 2D). The area under 2θ = 31.9° peak did not appear as broad as that seen in the XRD patterns of amorphous PMMA and SBF-mediated CaP deposition, suggesting that the crystallinity was mostly unaffected by the dip-coating and oxygen plasma treatment. By carrying out a 3-point bending test on the PMMA sheets, we found that the ultimate stress (p = 0.481) and strain at break (p = 0.279) were similar to the pristine PMMA (Figure 4A–C). Due to the presence of 30-to-50-µm-thick HAp layers laminating the PMMA surface [41], the coated PMMA was significantly stiffer than the pristine PMMA (p = 0.005) (Figure 4D).

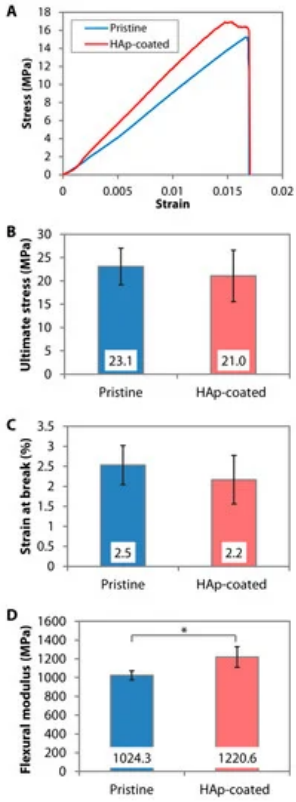

Figure 4. Mechanical properties of pristine and dip-coated PMMA. HAp nanoparticles were immobilized on the PMMA sheets via dip-coating. (**A**) Representative stress-strain curves generated from 3-point bending tests of the PMMA sheets. (**B**–**D**) Ultimate flexural stress, strain at break, and flexural modulus of pristine and dip-coated PMMA sheets. * p < 0.05.

References

1. Kokubo, T.; Takadama, H. How useful is SBF in predicting in vivo bone bioactivity? Biomaterials 2006, 27, 2907–2915, doi:10.1016/j.biomaterials.2006.01.017.
2. Kokubo, T.; Kushitani, H.; Sakka, S.; Kitsugi, T.; Yamamuro, T. Solutions able to reproducein vivo surface-structure cha nges in bioactive glass-ceramic A-W3. J. Biomed. Mater. Res. 1990, 24, 721–734, doi:10.1002/jbm.820240607.
3. Kokubo, T. Bioactive glass ceramics: properties and applications. Biomaterials 1991, 12, 155–163, doi:10.1016/0142-9 612(91)90194-f.
4. Tas, A.C. Synthesis of biomimetic Ca-hydroxyapatite powders at 37 °C in synthetic body fluids. Biomaterials 2000, 21, 1429–1438, doi:10.1016/s0142-9612(00)00019-3.
5. Takadama, H.; Hashimoto, M.; Mizuno, M.; Kokubo, T. Round-Robin Test of SBF For In Vitro Measurement of Apatite-F orming Ability of Synthetic Materials. Phosphorus Res. Bull. 2004, 17, 119–125, doi:10.3363/prb1992.17.0_119.

6. Oyane, A.; Onuma, K.; Ito, A.; Kim, H.-M.; Kokubo, T.; Nakamura, T. Formation and growth of clusters in conventional a nd new kinds of simulated body fluids. J. Biomed. Mater. Res. 2003, 64, 339–348, doi:10.1002/jbm.a.10426.
7. Kim, H.-M.; Miyazaki, T.; Kokubo, T.; Nakamura, T. Revised Simulated Body Fluid. Key Eng. Mater. 2000, 192, 47–50, d oi:10.4028/www.scientific.net/kem.192-195.47.
8. Lin, Z.; Zhao, X.; Chen, S.; Du, C. Osteogenic and tenogenic induction of hBMSCs by an integrated nanofibrous scaffol d with chemical and structural mimicry of the bone–ligament connection. J. Mater. Chem. B 2017, 5, 1015–1027, doi:1 0.1039/c6tb02156e.
9. Tanahashi, M.; Yao, T.; Kokubo, T.; Minoda, M.; Miyamoto, T.; Nakamura, T.; Yamamura, T. Apatite coated on organic p olymers by biomimetic process: Improvement in its adhesion to substrate by glow-discharge treatment. J. Biomed. Mat er. Res. 1995, 29, 349–357, doi:10.1002/jbm.820290310.
10. Tas, A.C.; Bhaduri, S.B. Rapid coating of Ti6Al4V at room temperature with a calcium phosphate solution similar to 10× simulated body fluid. J. Mater. Res. 2004, 19, 2742–2749, doi:10.1557/jmr.2004.0349.
11. Tanahashi, M.; Matsuda, T. Surface functional group dependence on apatite formation on self-assembled monolayers i n a simulated body fluid. J. Biomed. Mater. Res. 1997, 34, 305–315, doi:10.1002/(SICI)1097-4636(19970305)34:3<30 5::AID-JBM5>3.0.CO;2-O.
12. Leonor, I.B.; Kim, H.-M.; Carmona, D.; Kawashita, M.; Reis, R.L.; Kokubo, T.; Nakamura, T. Functionalization of differen t polymers with sulfonic groups as a way to coat them with a biomimetic apatite layer. J. Mater. Sci. Mater. Electron. 20 07, 18, 1923–1930, doi:10.1007/s10856-007-3106-6.
13. Kawai, T.; Ohtsuki, C.; Kamitakahara, M.; Miyazaki, T.; Tanihara, M.; Sakaguchi, Y.; Konagaya, S. Coating of an apatite layer on polyamide films containing sulfonic groups by a biomimetic process. Biomaterials 2004, 25, 4529–4534, doi:1 0.1016/j.biomaterials.2003.11.039.
14. Wentrup-Byrne, E.; Suzuki, S.; Grøndahl, L. CHAPTER 9. Biomedical Applications of Phosphorus-Containing Polymer s. In Polymer Chemistry Series; Royal Society of Chemistry (RSC): London, UK, 2014; pp.: 167–209.
15. Tretinnikov, O.N.; Kato, K.; Ikada, Y. In vitro hydroxyapatite deposition onto a film surface-grafted with organophosphat e polymer. J. Biomed. Mater. Res. 1994, 28, 1365–1373, doi:10.1002/jbm.820281115.
16. Hamai, R.; Maeda, H.; Sawai, H.; Shirosaki, Y.; Kasuga, T.; Miyazaki, T. Structural effects of phosphate groups on apati te formation in a copolymer modified with Ca2+ in a simulated body fluid. J. Mater. Chem. B 2017, 6, 174–182, doi:10.1 039/c7tb02363d.
17. Stancu, I.; Filmon, R.; Cincu, C.; Marculescu, B.; Zaharia, C.; Tourmen, Y.; Baslé, M.; Chappard, D. Synthesis of metha cryloyloxyethyl phosphate copolymers and in vitro calcification capacity. Biomaterials 2004, 25, 205–213, doi:10.1016/s 0142-9612(03)00485-x.
18. Mahjoubi, H.; Kinsella, J.M.; Murshed, M.; Cerruti, M. Surface Modification of Poly(d,l-Lactic Acid) Scaffolds for Orthope dic Applications: A Biocompatible, Nondestructive Route via Diazonium Chemistry. ACS Appl. Mater. Interfaces 2014, 6, 9975–9987, doi:10.1021/am502752j.
19. Sailaja, G.; Sreenivasan, K.; Yokogawa, Y.; Kumary, T.; Varma, H. Bioinspired mineralization and cell adhesion on surfa ce functionalized poly(vinyl alcohol) films. Acta Biomater. 2009, 5, 1647–1655, doi:10.1016/j.actbio.2008.12.005.
20. Cui, W.; Li, X.; Xie, C.; Zhuang, H.; Zhou, S.; Weng, J. Hydroxyapatite nucleation and growth mechanism on electrospu n fibers functionalized with different chemical groups and their combinations. Biomaterials 2010, 31, 4620–4629, doi:1 0.1016/j.biomaterials.2010.02.050.
21. Wang, L.; Jeong, K.J.; Chiang, H.H.; Zurakowski, D.; Behlau, I.; Chodosh, J.; Dohlman, C.H.; Langer, R.; Kohane, D.S. Hydroxyapatite for Keratoprosthesis Biointegration. Investig. Opthalmol. Vis. Sci. 2011, 52, 7392–7399, doi:10.1167/iov s.11-7601.
22. Riau, A.K.; Mondal, D.; Yam, G.H.F.; Setiawan, M.; Liedberg, B.; Venkatraman, S.S.; Mehta, J.S.; Venkatraman, S.S. S urface Modification of PMMA to Improve Adhesion to Corneal Substitutes in a Synthetic Core–Skirt Keratoprosthesis. A CS Appl. Mater. Interfaces 2015, 7, 21690–21702, doi:10.1021/acsami.5b07621.
23. Gadaleta, S.J.; Paschalis, E.P.; Betts, F.; Mendelsohn, R.; Boskey, A.L. Fourier transform infrared spectroscopy of the s olution-mediated conversion of amorphous calcium phosphate to hydroxyapatite: New correlations between X-ray diffra ction and infrared data. Calcif. Tissue Int. 1996, 58, 9–16, doi:10.1007/bf02509540.
24. Permyakova, E.S.; Kiryukhantsev-Korneev, P.V.; Gudz, K.Y.; Konopatsky, A.S.; Polčák, J.; Zhitnyak, I.Y.; Gloushankov a, N.A.; Shtansky, D.; Manakhov, A. Comparison of Different Approaches to Surface Functionalization of Biodegradable Polycaprolactone Scaffolds. Nanomaterials 2019, 9, 1769, doi:10.3390/nano9121769.
25. Murphy, W.; Hsiong, S.; Richardson, T.; Simmons, C.A.; Mooney, D. Effects of a bone-like mineral film on phenotype of adult human mesenchymal stem cells in vitro. Biomaterials 2005, 26, 303–310, doi:10.1016/j.biomaterials.2004.02.034.

26. Oyane, A.; Uchida, M.; Choong, C.; Triffitt, J.; Jones, J.; Ito, A. Simple surface modification of poly(ε-caprolactone) for a patite deposition from simulated body fluid. Biomaterials 2005, 26, 2407–2413, doi:10.1016/j.biomaterials.2004.07.048.
27. Qu, X.; Cui, W.; Yang, F.; Min, C.; Shen, H.; Bei, J.; Wang, S. The effect of oxygen plasma pretreatment and incubation in modified simulated body fluids on the formation of bone-like apatite on poly(lactide-co-glycolide) (70/30). Biomater. 2007, 28, 9–18, doi:10.1016/j.biomaterials.2006.08.024.
28. Şeker, U. Özgür Şafak; Demir, H.V. Material Binding Peptides for Nanotechnology. Molecules 2011, 16, 1426–1451, doi:10.3390/molecules16021426.
29. Care, A.; Bergquist, P.L.; Sunna, A. Solid-binding peptides: smart tools for nanobiotechnology. Trends Biotechnol. 2015, 33, 259–268, doi:10.1016/j.tibtech.2015.02.005.
30. Iijima, K.; Nagahama, H.; Takada, A.; Sawada, T.; Serizawa, T.; Hashizume, M. Surface functionalization of polymer substrates with hydroxyapatite using polymer-binding peptides. J. Mater. Chem. B 2016, 4, 3651–3659, doi:10.1039/c6tb00624h.
31. Kumada, Y.; Murata, S.; Ishikawa, Y.; Nakatsuka, K.; Kishimoto, M. Screening of PC and PMMA-binding peptides for site-specific immobilization of proteins. J. Biotechnol. 2012, 160, 222–228, doi:10.1016/j.jbiotec.2012.02.010.
32. Lee, H.; Dellatore, S.M.; Miller, W.M.; Messersmith, P.B. Mussel-Inspired Surface Chemistry for Multifunctional Coatings. Science 2007, 318, 426–430, doi:10.1126/science.1147241.
33. Ghorbani, F.; Zamanian, A.; Sahranavard, M. Mussel-inspired polydopamine-mediated surface modification of freeze-cast poly (ε-caprolactone) scaffolds for bone tissue engineering applications. Biomed. Tech. Eng. 2020, 65, 273–287, doi:10.1515/bmt-2019-0061.
34. Zhang, K.; Wang, Y.; Sun, T.; Wang, B.; Zhang, H.; Yi, W. Bioinspired Surface Functionalization for Improving Osteogenesis of Electrospun Polycaprolactone Nanofibers. Langmuir 2018, 34, 15544–15550, doi:10.1021/acs.langmuir.8b03357.
35. Ryu, J.; Ku, S.H.; Lee, H.; Park, C.B. Mussel-Inspired Polydopamine Coating as a Universal Route to Hydroxyapatite Crystallization. Adv. Funct. Mater. 2010, 20, 2132–2139, doi:10.1002/adfm.200902347.
36. Perikamana, S.K.M.; Shin, Y.M.; Lee, J.K.; Bin Lee, Y.; Heo, Y.; Ahmad, T.; Park, S.Y.; Shin, J.; Park, K.M.; Jung, H.S.; et al. Graded functionalization of biomaterial surfaces using mussel-inspired adhesive coating of polydopamine. Colloids Surfaces B Biointerfaces 2017, 159, 546–556, doi:10.1016/j.colsurfb.2017.08.022.
37. Li, J.; Liao, H.; Sjöström, M. Characterization of calcium phosphates precipitated from simulated body fluid of different buffering capacities. Biomaterials 1997, 18, 743–747, doi:10.1016/s0142-9612(96)00206-2.
38. Qu, H.; Wei, M. The effect of temperature and initial pH on biomimetic apatite coating. J. Biomed. Mater. Res. Part B Appl. Biomater. 2008, 87, 204–212, doi:10.1002/jbm.b.31096.
39. Malakauskaite-Petruleviciene, M.; Stankeviciute, Z.; Beganskiene, A.; Kareiva, A. Sol–gel synthesis of calcium hydroxyapatite thin films on quartz substrate using dip-coating and spin-coating techniques. J. Sol-Gel Sci. Technol. 2014, 71, 437–446, doi:10.1007/s10971-014-3394-5.
40. Deng, X.; Hao, J.; Wang, C. Preparation and mechanical properties of nanocomposites of poly(D,L-lactide) with Ca-deficient hydroxyapatite nanocrystals. Biomaterials 2001, 22, 2867–2873, doi:10.1016/s0142-9612(01)00031-x.
41. Riau, A.K.; Mondal, D.; Setiawan, M.; Palaniappan, A.; Yam, G.H.F.; Liedberg, B.; Venkatraman, S.S.; Mehta, J.S. Functionalization of the Polymeric Surface with Bioceramic Nanoparticles via a Novel, Nonthermal Dip Coating Method. ACS Appl. Mater. Interfaces 2016, 8, 35565–35577, doi:10.1021/acsami.6b12371.
42. Riau, A.K.; Lwin, N.C.; Gelfand, L.; Hu, H.; Liedberg, B.; Chodosh, J.; Venkatraman, S.S.; Mehta, J.S. Surface modification of corneal prosthesis with nano-hydroxyapatite to enhance in vivo biointegration. Acta Biomater. 2020, 107, 299–312, doi:10.1016/j.actbio.2020.01.023.